PHYSICAL REVIEW E **79**, 065304(R) (2009)

Two different kinds of rogue waves in weakly crossing sea states

V. P. Ruban
Landau Institute for Theoretical Physics, 2 Kosygin Street, 119334 Moscow, Russia
(Received 27 March 2009; published 16 June 2009)

Formation of giant waves in sea states with two spectral maxima centered at close wave vectors $\mathbf{k}_0 \pm \Delta\mathbf{k}/2$ in the Fourier plane is numerically simulated using the fully nonlinear model for long-crested water waves [V. P. Ruban, Phys. Rev. E **71**, 055303(R) (2005)]. Depending on an angle θ between the vectors $\mathbf{k}_0$ and $\Delta\mathbf{k}$, which determines a typical orientation of interference stripes in the physical plane, rogue waves arise having different spatial structure. If $\theta \lesssim \arctan(1/\sqrt{2})$, then typical giant waves are relatively long fragments of essentially two-dimensional (2D) ridges, separated by wide valleys and consisting of alternating oblique crests and troughs. At nearly perpendicular $\mathbf{k}_0$ and $\Delta\mathbf{k}$, the interference minima develop to coherent structures similar to the dark solitons of the nonlinear Schrodinger equation, and a 2D freak wave looks much as a piece of a one-dimensional freak wave bounded in the transversal direction by two such dark solitons.

DOI: 10.1103/PhysRevE.79.065304 PACS number(s): 47.35.Bb, 92.10.−c, 02.60.Cb

The problem of extreme ocean waves (known as freak waves, rogue waves, or killer waves) has attracted much attention in recent years (see, e.g., the reviews [1,2], where different physical mechanisms of the rogue wave phenomenon are discussed and many related works are referenced; for some recent developments in this field, see Refs. [3–17]). With a typical background wave amplitude $A_0 \approx [0.015, \ldots, 0.02]\lambda_0$ (where $\lambda_0 = 2\pi/k_0$ is a typical wavelength), the maximum elevation of a freak wave can reach a height $Y_{\max} > 0.06\lambda_0$, which approaches the limiting Stokes wave. Profiles of freak waves are very steep, and they strongly deviate from the sinusoidal shape. In different circumstances, the giant waves can be caused by different reasons. Accordingly, there are several probable scenarios explaining formation of these waves. It has been recognized that one of the most important reasons for freak waves is the modulational Benjamin-Feir-Zakharov instability taking place in relatively long and high groups of propagating waves [18,19]. Efficiency of this mechanism is usually characterized by the so-called Benjamin-Feir index [4], (BFI) $\sim \lambda_0^{-2} A_0 l_0$, where l_0 is a typical length of wave groups. For example, in completely incoherent sea states (low BFI) the modulational instability is suppressed, and rather rare appearance of anomalous wave events is basically of a purely kinematic origin. This limit is well described by the approximation of noninteracting normal wave modes renormalized by a weakly nonlinear transformation excluding three-wave (nonresonant) processes (see, e.g., Refs. [2,5,20] and references therein). Higher values of BFI correspond to more favorable conditions for the occurrence of freak waves. Nonlinear wave interactions become essential so giant waves arise in the process of evolution of some coherent structures. In particular, the limit of infinitely high BFI (a weakly disturbed planar wave as an initial state) has been recently studied in works [8,9], and specific zigzag-shaped obliquely oriented wave stripes were found to develop in the nonlinear stage of the modulational instability, with rogue waves occurring mainly at zigzag turns. That case roughly corresponds to another probable scenario when refraction of swell in a spatially nonuniform current causes preliminary amplification of wave height around caustic region [21,22]. A different kind of coherent structures has been recognized recently for purely one-dimensional (1D) waves (planar flows), the so-called giant breathers [10], which are extremely short and steep envelope solitons, containing just 1–2 waves.

Thus, though BFI is definitely a relevant parameter, but in some situations it does not completely characterize freak waves as it takes place, for example, for 1D waves [10–13] or for long-crested waves in contrast to short-crested waves [14,15] or in crossing sea states [16,17]. The reason is that coherent wave structures depend on additional parameters as well. In the present work, we investigate this question in more detail for weakly crossing sea states. More specifically, we consider sea states with two spectral peaks centered at wave vectors $\mathbf{k}_{1,2} = \mathbf{k}_0 \mp \Delta\mathbf{k}/2$ in the Fourier plane, and we assume $|\Delta\mathbf{k}| \ll |\mathbf{k}_0|$. Thus, an angle of incidence α between $\mathbf{k}_1$ and $\mathbf{k}_2$ is small in our study. Such a situation corresponds to the presence of relatively long and wide wave stripes obliquely oriented to the wave fronts in a range of angles near the angle θ between the vectors $\Delta\mathbf{k}$ and $\mathbf{k}_0$. We study numerically how the process of rogue wave formation depends on the angle θ. The computations are based on the approximate theoretical model for long-crested fully nonlinear water waves developed in Refs. [23,24] and later successfully applied in Refs. [8,9]. The model is of the first-order accuracy in a small parameter $\epsilon \sim \alpha^2 \ll 1$, and it is intermediate between the exact Eulerian dynamics and the approximate equations for wave envelopes [generalizations of the nonlinear Schrodinger equation (NLSE)] suggested in Refs. [25–27]. It should be emphasized that our method makes possible to compute profiles of individual abnormal waves for $\alpha^2 \ll 1$, while in Refs. [16,17] only waves with smooth envelopes in crossing sea states for $\theta = \pi/2$ were studied, however for arbitrary α.

The main results of this work are the following. If $\theta \lesssim \arctan(1/\sqrt{2})$, then the nonlinearity is defocusing along the stripes and it is focusing across them. The situation is opposite at nearly perpendicular $\mathbf{k}_0$ and $\Delta\mathbf{k}$. Accordingly, rogue waves, occurring at the sea surface, are different in these two cases. In the first case, freak waves look as fragments of structures which are similar to the solitonic solutions of a focusing NLSE for a wave envelope. Such ex-

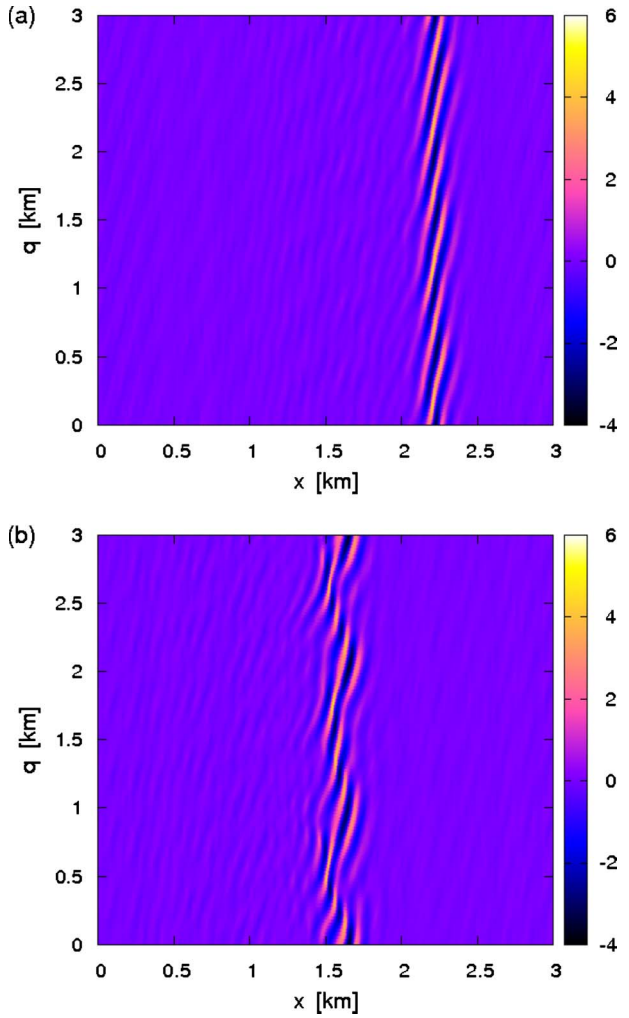

FIG. 1. (Color online) Evolution of a perturbed high-amplitude oblique soliton into a zigzag structure: (a) surface elevation, in meters, at $t=17$ min and 26.5 s and (b) surface elevation at $t=23$ min and 35.9 s.

tremely narrow and steep solitons are in essence rows of alternating oblique crests and troughs [see Fig. 1(a)]. When perturbed by a weak two-dimensional (2D) random field, the oblique solitons can exist for many wave periods almost unchanged, but later they transform to zigzag structures similar to that described in Ref. [9] (see Figs. 1 and 2, for example). It should be noted that in the limit $\theta \to 0$ such extreme oblique solitons coincide with the recently discovered 1D giant breathers [10]. Thus, the fundamental role of these coherent structures in the dynamics of water waves is confirmed. At nearly perpendicular $\mathbf{k}_0$ and $\Delta\mathbf{k}$, another kind of coherent structures comes into play, similar to the dark solitons of a defocusing NLSE. Dark solitons develop at the interference minima and they transversally separate wave groups subjected to the longitudinal modulational instability. Freak waves in this case have nearly 1D profiles, but they are bounded in the transversal direction by two dark solitons.

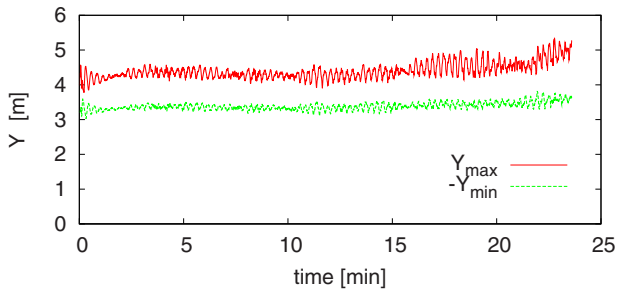

FIG. 2. (Color online) Global maximum and minimum elevation of the oblique soliton vs time.

To understand better numerical results, it is useful to have in mind a qualitative model describing weakly nonlinear water waves in terms of a complex wave amplitude $A(x_1,x_2,t)$, which determines the free surface elevation as follows:

$$Y(x_1,x_2,t) \approx \mathrm{Re}[A(x_1,x_2,t)\exp(ik_0x_1 - i\omega_0 t)], \qquad (1)$$

where (x_1,x_2) are horizontal coordinates, with x_1 axis along $\mathbf{k}_0$, $\omega_0=(gk_0)^{1/2}$ is frequency of the carrier wave, and g is the gravity acceleration. The function A is known to approximately obey a 2D NLSE [18],

$$\frac{i}{\omega_0}\frac{\partial A}{\partial t} + \frac{i}{2k_0}\frac{\partial A}{\partial x_1} = \frac{1}{8k_0^2}\left(\frac{\partial^2 A}{\partial x_1^2} - 2\frac{\partial^2 A}{\partial x_2^2}\right) + \frac{k_0^2}{2}|A|^2 A. \qquad (2)$$

The oblique stripes roughly correspond to the following 1D reductions in Eq. (2):

$$A = k_0^{-1}\Psi(\xi,\tau), \quad \xi = k_0[(x_1 - V_{\mathrm{gr}}t)\cos\theta + x_2 \sin\theta], \qquad (3)$$

where $\tau=\omega_0 t$ and $V_{\mathrm{gr}}=(\omega_0/2k_0)$ is the group velocity. As a result, we have a 1D NLSE describing the transversal dynamics of idealized, infinitely long wave stripes,

$$i\Psi_\tau = \frac{1}{4}[(1/2)\cos^2\theta - \sin^2\theta]\Psi_{\xi\xi} + \frac{1}{2}|\Psi|^2\Psi. \qquad (4)$$

Depending on the sign of the dispersion coefficient $D(\theta)=[(1/2)\cos^2\theta - \sin^2\theta]$, this is either focusing equation or defocusing one, and the dynamics is quite different in each case. For example, in the focusing case (when $D>0$), the nonlinearity can become saturated with the so-called (bright) solitons,

$$\Psi_{\mathrm{bs}} = \frac{s}{\cosh[(s/\sqrt{D})(\xi - \xi_0)]}\exp(-i\tau s^2/4 + i\phi_0), \qquad (5)$$

where s is a wave steepness and ξ_0 and ϕ_0 are arbitrary constants. These solutions describe infinitely long wave ridges consisting of alternating oblique crests and troughs. Physical conditions of applicability of the above formula imply $s \lesssim 0.1$ and $s/\sqrt{D} \ll 1$, but actually these solutions have been found to continue qualitatively to considerably higher values $s \lessapprox 0.27$. We specially studied a long-time behavior of such extreme solitons both for $\theta=0$ (the giant breathers at 2D surface) and for $\theta \neq 0$. It is one of the main results of the present work that in two dimensions extreme solitons can exist for a long time before transformation into zigzag structures. An example of evolution of a perturbed high-amplitude oblique soliton is presented in Figs. 1 and 2 for $\lambda_0 \approx 100$ m, $\theta \approx \arctan(1/5)$, and $s \approx 0.22$.

In the defocusing case (when $D<0$), the so-called dark solitons are possible,

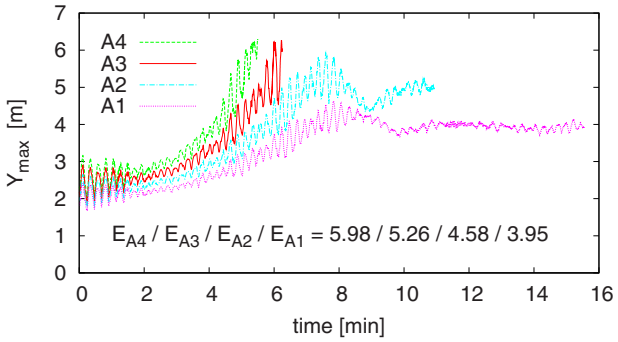

FIG. 3. (Color online) Maximum elevation of the free surface vs time in the numerical experiments A1–A4.

$$\Psi_{ds} = s\ \tanh[(s/\sqrt{-D})(\xi - \xi_0)]\exp(-i\tau s^2/2 + i\phi_0), \quad (6)$$

which separate two domains of opposite amplitude.

In view of the above, it is clear that since the effective dispersion coefficient $D(\theta)$ changes the sign at $\theta_* = \arctan(1/\sqrt{2})$, in the full 2D dynamics of random wave fields there should be two substantially different regimes, one regime at $\theta \lesssim \theta_*$ and another at θ close to $\pi/2$. This hypothesis is confirmed in general by numerical experiments reported here.

The computations were performed in the dimensionless square domain $2\pi \times 2\pi$ with periodic boundary conditions along horizontal coordinates x and q (see Refs. [23,24] for details). Thus, all the discrete Fourier modes correspond to dimensionless integer wave vectors $\mathbf{k}=(k,m)$. The vector $\mathbf{k}_0$ (and x_1 axis) was generally taken slightly different from the direction of x axis in order to take into account the effect of gradual reorientation of wave crests along the oblique stripes (see Ref. [9]). Final results were rescaled to give a convenient for presentation value $\lambda_0 \approx 100$ m, which is quite typical in natural sea conditions. The corresponding wave period is $T_0 = [2\pi\lambda_0/g]^{1/2} \approx 8$ s. Two small sets of typical numerical

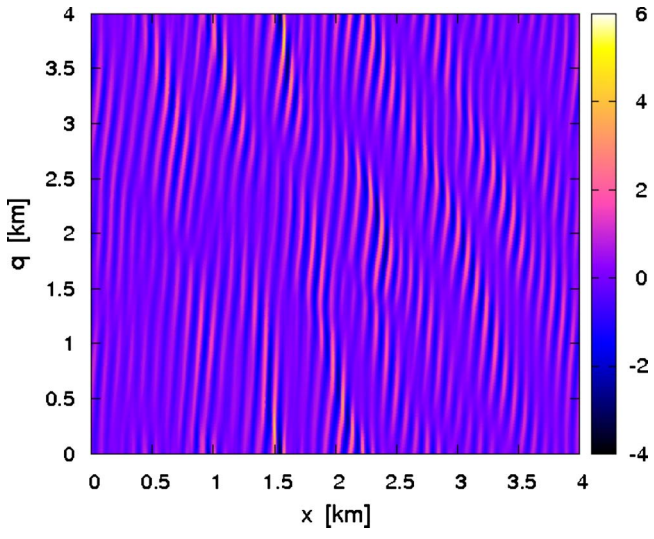

FIG. 4. (Color online) Experiment A3, $t=6$ min and 2.5 s: the two big waves are at $x \approx 1.6$ km, $q \approx [3.7, \ldots, 3.9]$ km and at $x \approx 1.5$ km, $q \approx [0.1, \ldots, 0.3]$ km.

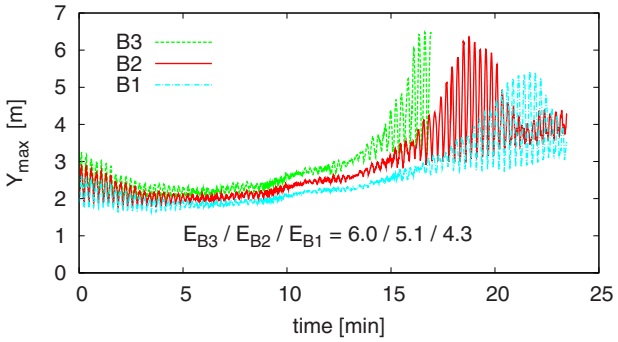

FIG. 5. (Color online) Maximum elevation of the free surface in the numerical experiments B1–B3.

experiments are presented, designated as A1–A4 and B1–B3. Within each set, at $t=0$ the normal Fourier modes of the wave field were taken in the form $a_{km}(0) = cF(k,m)\exp(i\gamma_{km})$, with a positive function $F(k,m)$ having two nearly Gaussian maxima at $\mathbf{k}_0 \pm \Delta\mathbf{k}/2$ and with quasirandom initial phases γ_{km} different for A and for B. In each experiment a choice of the coefficient c gave different values of the total energy $E_{A1}, E_{A2}, E_{A3}, E_{A4}$ and E_{B1}, E_{B2}, E_{B3}. In set A we took $\mathbf{k}_0 = (40.0, -2.5)$ and $\Delta\mathbf{k} = (7.0, 2.0)$, so a case $\theta < \theta_*$ was simulated, while in set B it was a crossing sea state with $\theta = \pi/2$: $\mathbf{k}_0 \pm \Delta\mathbf{k}/2 = (39.5, \pm 3.5)$.

For set A, some results are presented in Figs. 3 and 4. The modulational instability acts in this case from the very beginning, and it needs a short time 5–8 min to produce freak waves in the initially most tall wave groups. The two neighboring big waves in Fig. 4 look as a fragment of an oblique soliton [compare to Fig. 1(a)]. The computations A4 and A3 were terminated at the moments when the freak waves broke, while in experiments A2 and A1 the waves remained smooth, so at later times nearly stationary long oblique solitons were observed (not shown).

Results of experiments B1–B3 (see Figs. 5–7) are more intriguing since there were two stages in the evolution of the wave field before rogue waves arose. In the first stage, for

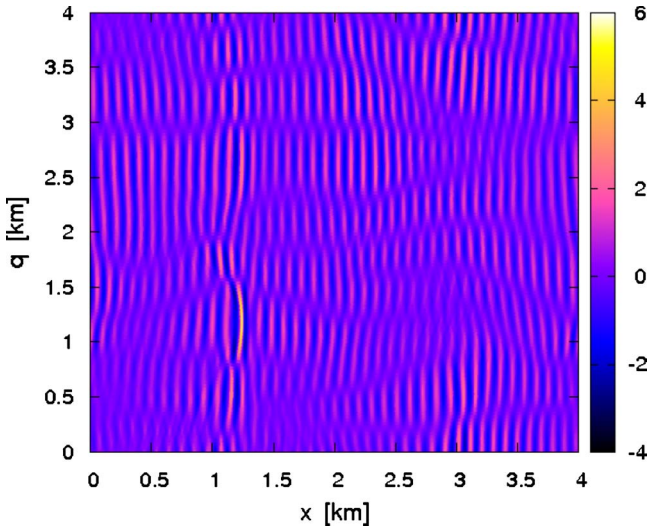

FIG. 6. (Color online) Experiment B2, $t=18$ min 43.8 s: the rogue wave is at $x \approx 1.2$ km and $q \approx [1.0, \ldots, 1.3]$ km.

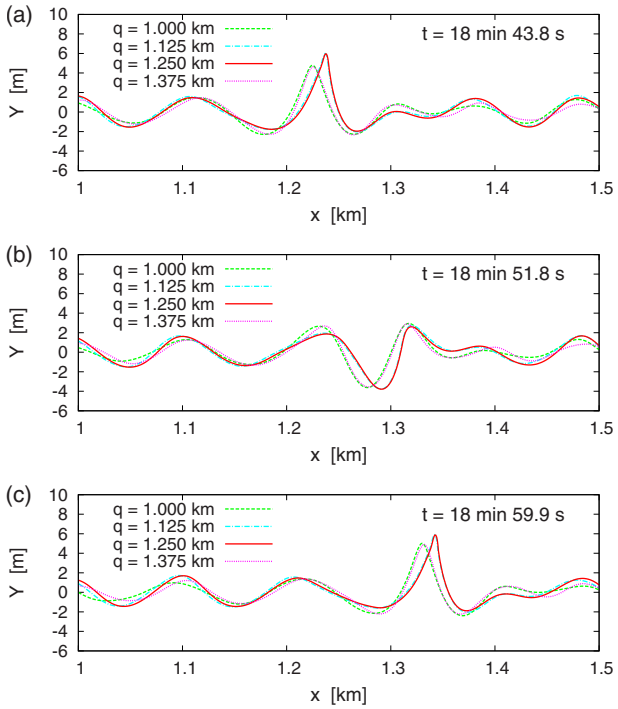

FIG. 7. (Color online) (a) Profiles of the freak wave from Fig. 6; (b) 8 s later: "a hole in the sea;" and (c) 16 s later: the big wave has risen again.

4–7 min after the beginning, it was the formation of dark solitons along interference minima, which the process was accompanied by substantial decrease in wave amplitude along interference maxima. At the end of this stage, the free surface has been divided by dark solitons into domains of nearly 1D dynamics. In the second stage, adjacent domains interact in a complicated manner, and in one of them the amplitude increases, resulting in fast development of the longitudinal modulational instability. As the result, a single rogue wave grows, which is squeezed from the lateral sides between two dark solitons, as shown in Fig. 6. The rogue wave is "breathing," with time-alternating tall crest and deep trough, and it approximately repeats the profile after $2T_0$ (see Fig. 7). After a dozen of the oscillations, the big wave spreads in the transversal direction and disappears (not shown).

As results A and B are compared, it becomes clear that the unusual properties of the abnormal waves in weakly crossing seas are more prominent when the interference stripes are nearly perpendicular to the wave crests.

These investigations were supported by RFBR (Grants No. 09-01-00631 and No. 07-01-92165), by the Leading Scientific Schools of Russia Grant No. 4887.2008.2, and by the Program "Fundamental Problems of Nonlinear Dynamics" from the RAS Presidium.

[1] C. Kharif and E. Pelinovsky, Eur. J. Mech. B/Fluids **22**, 603 (2003).
[2] K. Dysthe, H. E. Krogstad, and P. Muller, Annu. Rev. Fluid Mech. **40**, 287 (2008).
[3] Special Issue: Eur. J. Mech. B/Fluids **25**, 535 (2006).
[4] P. A. E. M. Janssen, J. Phys. Oceanogr. **33**, 863 (2003).
[5] F. Fedele and M. A. Tayfun, J. Fluid Mech. **620**, 221 (2009).
[6] C. Fochesato, S. Grilli, and F. Dias, Wave Motion **44**, 395 (2007).
[7] H. Socquet-Juglard, K. Dysthe, K. Trulsen, H. E. Krogstad, and J. Liu, J. Fluid Mech. **542**, 195 (2005).
[8] V. P. Ruban, Phys. Rev. E **74**, 036305 (2006).
[9] V. P. Ruban, Phys. Rev. Lett. **99**, 044502 (2007).
[10] A. I. Dyachenko and V. E. Zakharov, JETP Lett. **88**, 307 (2008).
[11] V. E. Zakharov, A. I. Dyachenko, and O. A. Vasilyev, Eur. J. Mech. B/Fluids **21**, 283 (2002).
[12] A. I. Dyachenko and V. E. Zakharov, Pis'ma Zh. Eksp. Teor. Fiz. **81**, 318 (2005); [JETP Lett. **81**, 255 (2005)].
[13] V. E. Zakharov, A. I. Dyachenko, and O. A. Prokofiev, Eur. J. Mech. B/Fluids **25**, 677 (2006).
[14] O. Gramstad and K. Trulsen, J. Fluid Mech. **582**, 463 (2007).
[15] M. Onorato, T. Waseda, A. Toffoli, L. Cavaleri, O. Gramstad, P. A. Janssen, T. Kinoshita, J. Monbaliu, N. Mori, A. R. Osborne, M. Serio, C. T. Stanberg, H. Tamura, and K. Trulsen, Phys. Rev. Lett. **102**, 114502 (2009).
[16] M. Onorato, A. R. Osborne, and M. Serio, Phys. Rev. Lett. **96**, 014503 (2006).
[17] P. K. Shukla, I. Kourakis, B. Eliasson, M. Marklund, and L. Stenflo, Phys. Rev. Lett. **97**, 094501 (2006).
[18] V. E. Zakharov, Sov. Phys. JETP **24**, 455 (1967).
[19] T. B. Benjamin and J. E. Feir, J. Fluid Mech. **27**, 417 (1967).
[20] M. A. Tayfun, J. Geophys. Res. **85**, 1548 (1980).
[21] D. H. Peregrine, Adv. Appl. Mech. **16**, 9 (1976).
[22] I. V. Lavrenov and A. V. Porubov, Eur. J. Mech. B/Fluids **25**, 574 (2006).
[23] V. P. Ruban, Phys. Rev. E **71**, 055303(R) (2005).
[24] V. P. Ruban and J. Dreher, Phys. Rev. E **72**, 066303 (2005).
[25] K. B. Dysthe, Proc. R. Soc. London, Ser. A **369**, 105 (1979).
[26] K. Trulsen and K. B. Dysthe, Wave Motion **24**, 281 (1996).
[27] K. Trulsen, I. Kliakhandler, K. B. Dysthe, and M. G. Velarde, Phys. Fluids **12**, 2432 (2000).